Excited-State Electronic Asymmetry Prevents Photoswitching in Terthiophene Compounds (Supporting Information)

Benjamin H. Strudwick,[*,†] Jing Zhang,[‡] Michiel F. Hilbers,[†] Wybren Jan Buma,[†] Sander Woutersen,[†] Sheng Hua Liu,[‡] and František Hartl[*,¶]

E-mail: b.h.strudwick@uva.nl; f.hartl@reading.ac.uk

[*]To whom correspondence should be addressed

[†]Molecular Photonics Group, Van 't Hoff Institute for Molecular Sciences, University of Amsterdam, Science Park 904, 1098 XH Amsterdam, The Netherlands

[‡]Key Laboratory of Pesticide and Chemical Biology, Ministry of Education, College of Chemistry, Central China Normal University, Wuhan 430079, P.R. China

[¶]Department of Chemistry, University of Reading, Whiteknights, Reading RG6 6AD, United Kingdom

Supporting Information

Table of Contents

S1. Photo-oxidisation of 1b Spectra

S2. Steady State Spectra

S3. UV/vis Transient Absorption Spectra of 1a

S4. DFT & TD-DFT Calculations

S5. Global Fitting for the Nanosecond Transient Absorption Spectra

S6. NMR & NOESY Spectra of 1a

S7. Femtosecond Transient Absorption Spectra of 1b in THF

S1. Photo-oxidisation of 1b Spectra

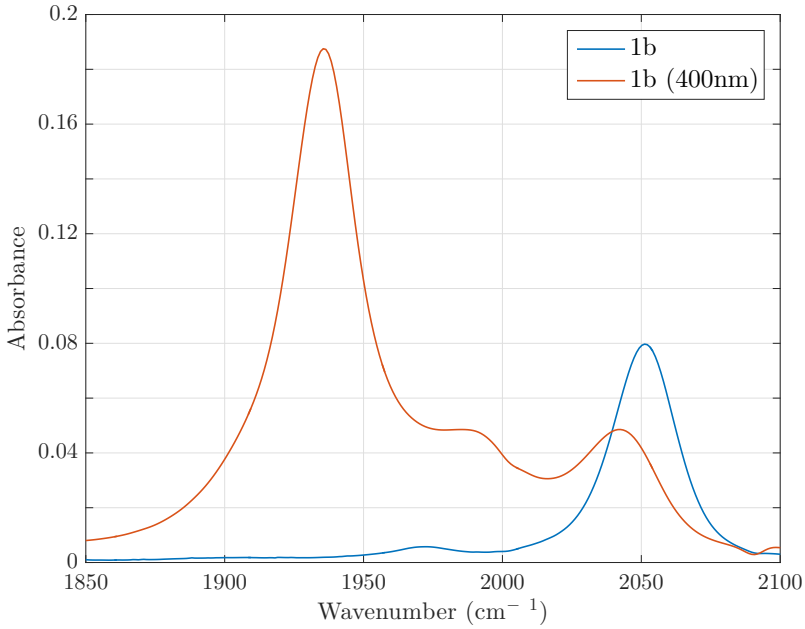

Figure S1: IR absorption spectra of **1b** in DCM before (blue) and after being irradiated with light ($\lambda = 400$ nm) for 5 minutes (red). The latter clearly demonstrates the formation of $\mathbf{1b}^{+}$.[S1]

The spectra shown in **Figures S1** and **S2** are IR absorption spectra (using a Bruker Vertex 70 FTIR spectrometer) of **1b** before and after irradiation with light ($\lambda = 400$ nm). **Figure S1** shows the spectral region of the ethynyl mode; after irradiation the three modes can be seen to separate. **Figure S2** shows the NIR spectral region where a strong electronic tranisition can be seen for the irradiated **1b**. The same sample was then measured in the UV/vis region, **Figure S3**, (using a Hewlett Packard 8453 UV/vis spectrophotometer) where a new species (at 720 nm) is easily distinguishable. The species formed was assigned to be $\mathbf{1b}^{+}$ comparing with the spectra from the spectro-electrochemical studies.[S1]

Figure S4 shows the time-resolved IR measurements of **1b** in DCM on a ps time scale. After irradiation with light ($\lambda = 400$ nm) **1b** converts to $\mathbf{1b}^{+}$ within the first nanosecond. The rapid oxidation rules out simple diffusion of photogenerated chlorine radicals, which would take place on the nanosecond time scale.

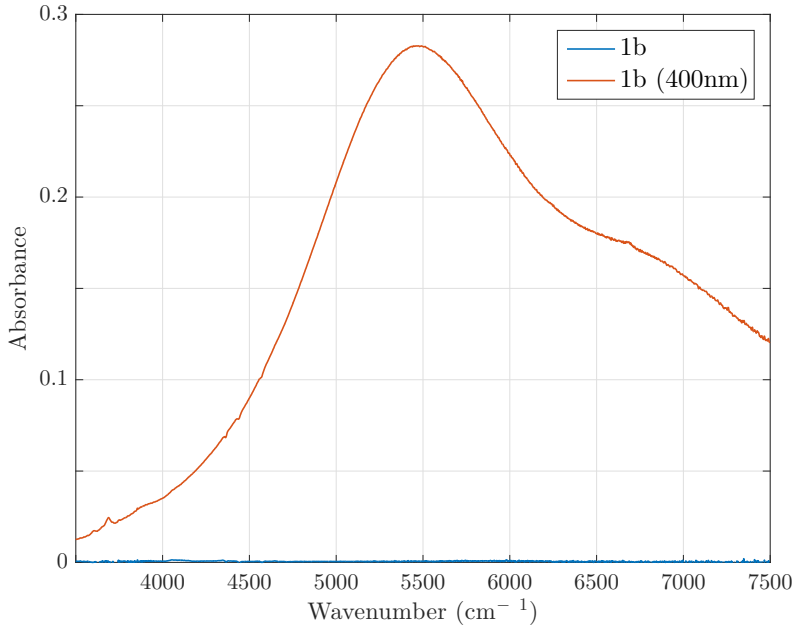

Figure S2: Electronic absorption spectra of **1b** in DCM before (blue) and after being irradiated with light ($\lambda = 400$ nm) for 5 minutes (red). The latter reproduces the NIR absorption of $\mathbf{1b}^{+}$.[S1]

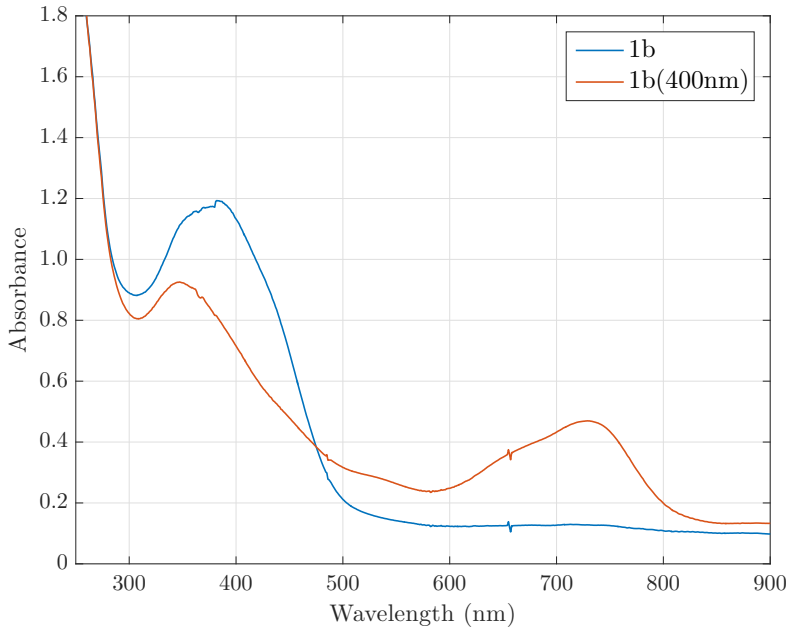

Figure S3: Steady state UV/vis spectra (using s Hewlett Packard 8453 UV/vis spectrophotometer) of **1b** in DCM before (blue) and after being irradiated with light ($\lambda = 400$ nm) for 5 minutes (red). The electronic absorption at 720 nm (red) belongs to $\mathbf{1b}^{+}$.[S1]

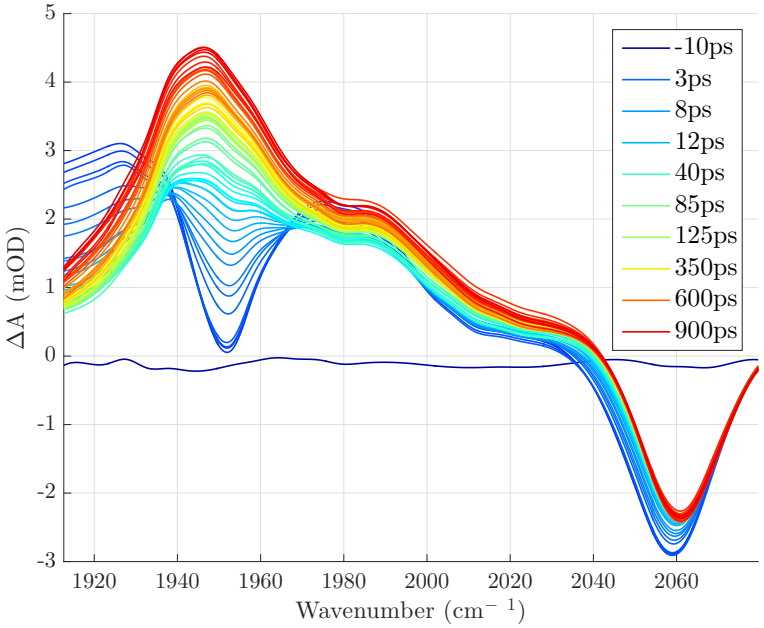

Figure S4: TR-IR spectra of **1b** in DCM, excited at ca. 400 nm, upon continual circulation of the solution to ensure a fresh sample.

S2. Steady State Spectra

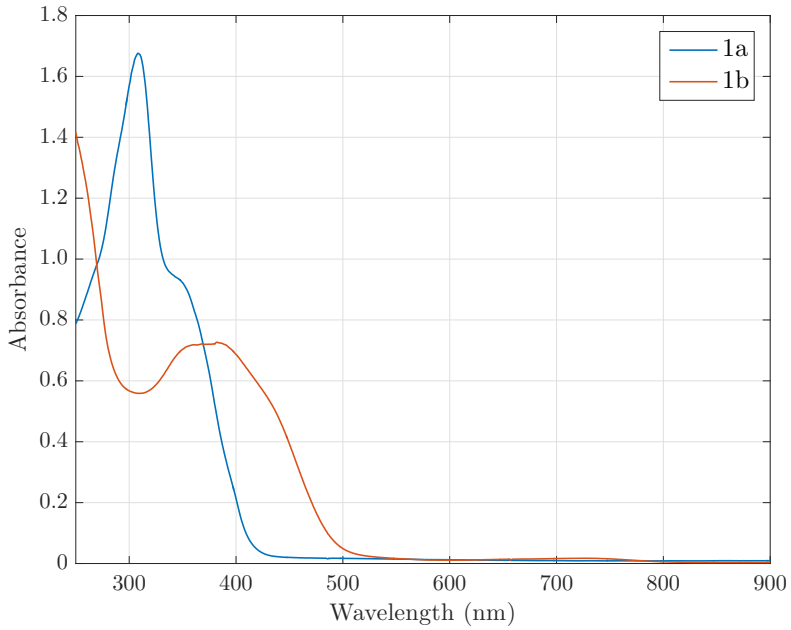

Figure S5: Steady-state UV/vis absorption spectra of **1a** and **1b** in THF (using a Hewlett Packard 8453 UV/vis spectrophotometer).

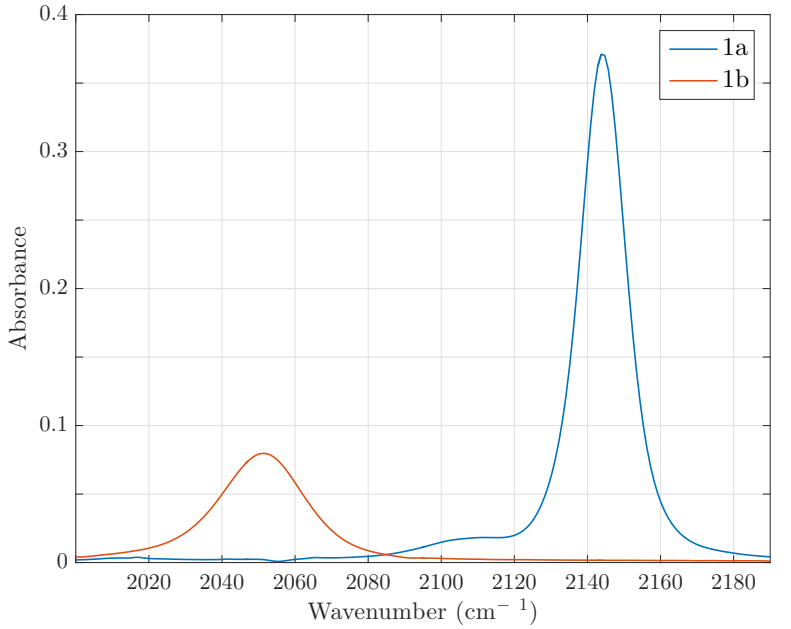

Figure S6: IR absorption spectra showing the ethynyl stretching modes of **1a** and **1b** in THF (using a Bruker Vertex 70 FTIR spectrometer).

S3. UV/vis Transient Absorption Spectra of 1a

UV/vis transient absorption spectra of **1a** in DCM, irradiated with light (λ = 400 nm), are shown in **Figures S7** and **S8**. The spectra show a final long lived state that lasts till the end of the accessible time range. This final feature can be continued to be followed in the nanosecond TA measurement, **Figure S8**, where **1a** returns to the GS. Comparing **Figures S7** and **S8** with the UV/vis TA experiments in THF, **Figures 3** and **4**, shows no difference between the decay pathway of **1a** in THF and DCM. **Figure S9** presents the decay-associated spectra of the picosecond UV/vis TA of **1a** in THF provided in **Figure 3**. There are three species seen within the first 4 ns after excitation; an initial species S* associated with the hot singlet state, the relaxed singlet state S and the triplet state T.

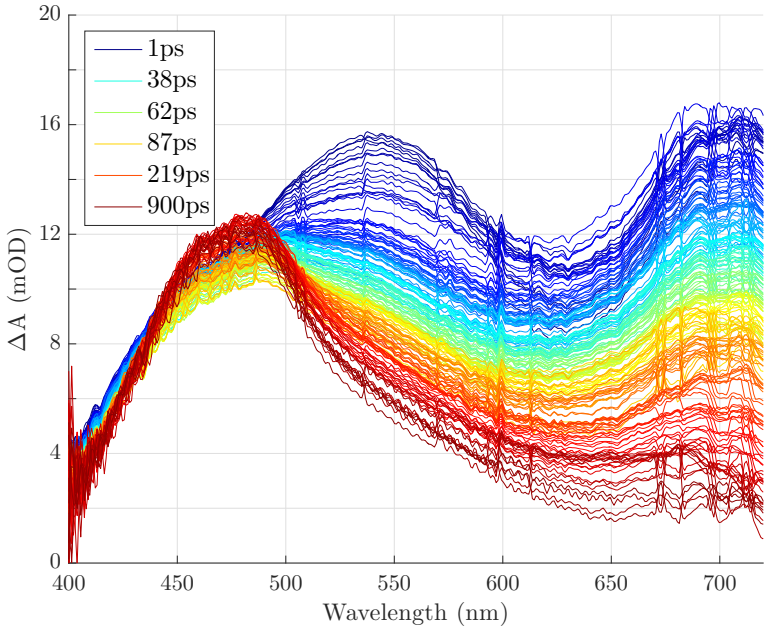

Figure S7: Femtosecond TA spectra of **1a** in DCM, excited at ca. 400 nm.

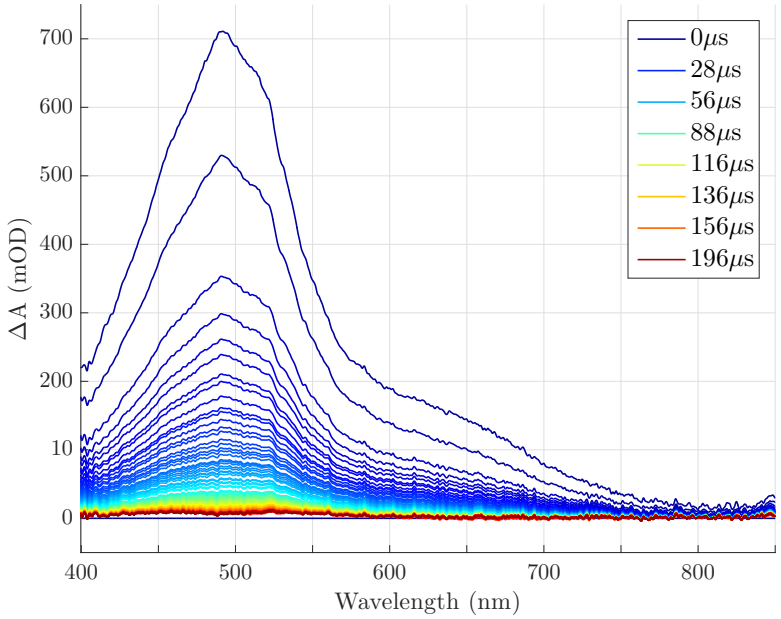

Figure S8: Nanosecond TA spectra of **1a** in DCM, excited at ca. 400 nm.

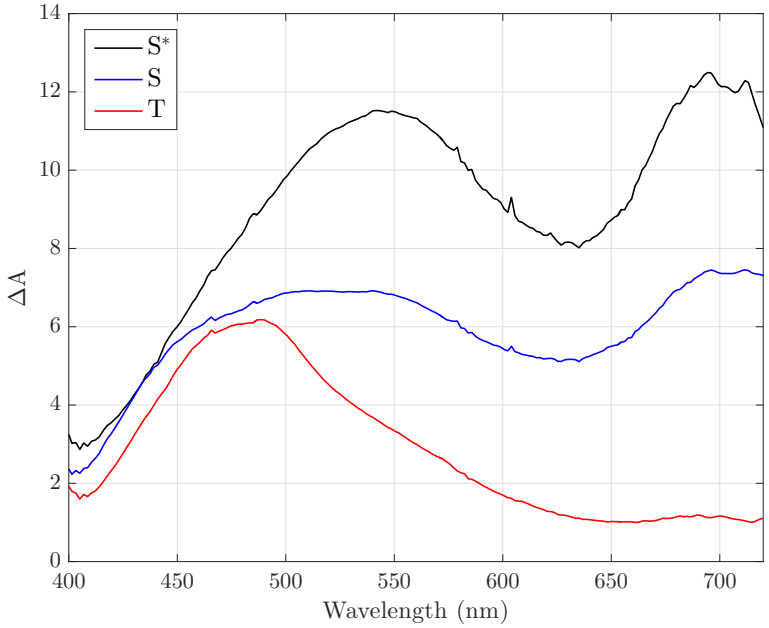

Figure S9: Femtosecond visible transient decay-associated spectra (DAS) of **1a** in THF, excited at ca. 400 nm. They refer to **Figure 3** in the main text.

S4. DFT & TD-DFT Calculations

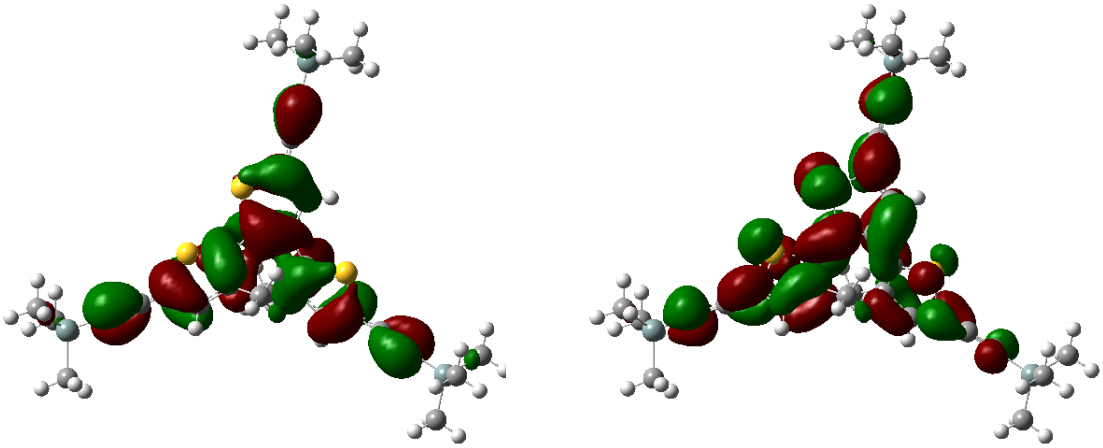

Figure S10: Left: The DFT-calculated HOMO of **1a**. Right: The DFT-calculated LUMO of **1a**. HOMO energy: -0.20363 a.u. (-5.54104 eV). LUMO energy: -0.07259 a.u. (-1.97527 eV). LUMO/HOMO gap: 0.13104 a.u. (3.56577 eV). Contour values: ± 0.02 (e borh^{-3})$^{1/2}$

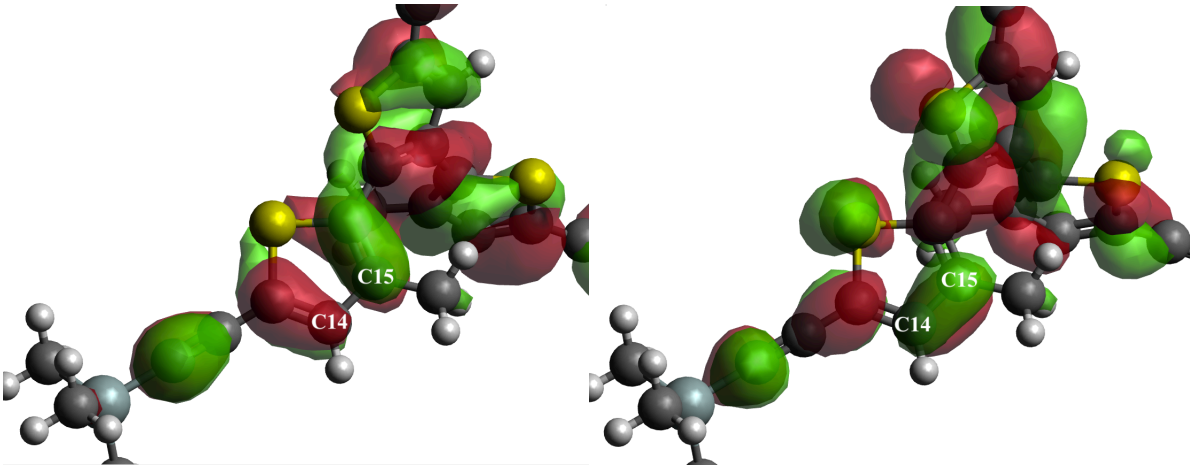

Figure S11: Left: The DFT-calculated HOMO of **1a**, focusing on the bond $C_{14}-C_{15}$ (white). Right: The DFT-calculated LUMO of **1a**, focusing on the bond $C_{14}-C_{15}$ (white).

Figure S10 shows the calculated HOMO and LUMO of **1a** in the ground state. The geometry optimisation of the ground state of **1a** was performed at the Density Functional Theory level using the B3LYP functional and the 6-31G(d,p) basis set. The Polarisable Continuum Model (PCM) was adopted to describe solvation effects (solvent: dichloromethane). The HOMO is symmetrically spread across the whole compound. The LUMO shows to be more asymmetric, that is, delocalized predominantly over **e1** and **e2**, in **Figure 1**. The 30 lowest electronic transitions of **1a** are shown in **Figure S13**. The stick spectra, shown in black, have been convoluted with a Gaussian to produce the predicted spectra shown in blue. The predicted spectra and the measured UV/vis spectra of **1a**, shown in **Figure S5**, are in good agreement. **Table S1** contains the bond lengths for each of the states of **1a**; the ground state, the singlet state and the triplet state. **Figure S11** shows the same HOMO and LUMO as in **Figure S10** however, focused on the bond $C_{14} - C_{15}$ (C_{15} is the potentially reactive carbon).The difference between the HOMO and LUMO points to a strong bond formation or a change in conjugation of this bond in the excited state.

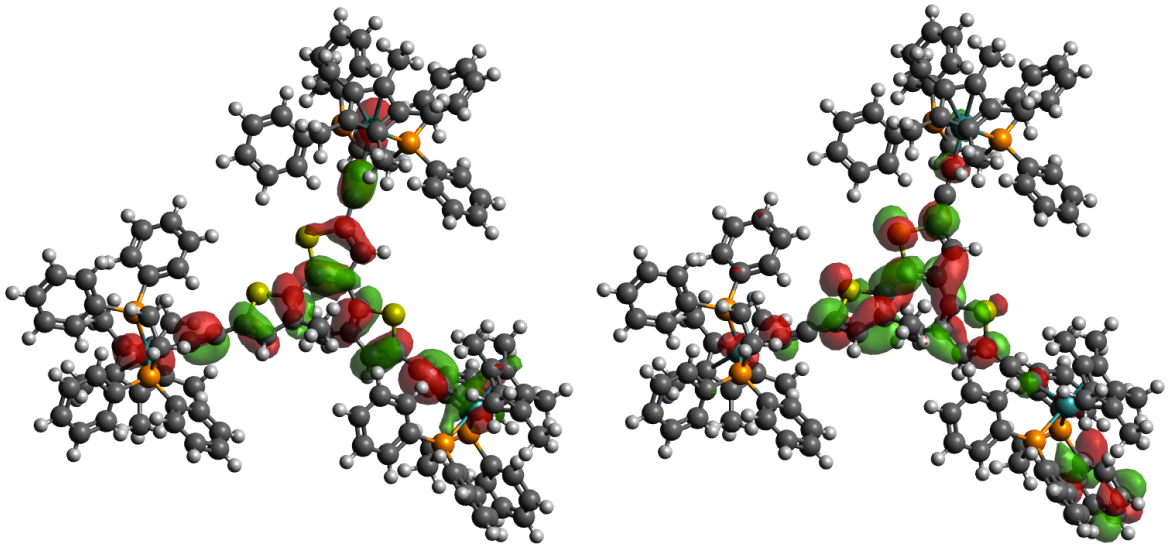

Figure S12: Left: The DFT-calculated HOMO of **1b**. Right: The DFT-calculated LUMO + 1 of **1b**. HOMO energy: -0.19068 a.u. (-5.18867 eV). LUMO + 1 energy: 0.01459 a.u. (0.397014 eV). LUMO + 1/HOMO gap: 0.20527 a.u. (5.5857 eV). Contour values: ± 0.02 (e borh^{-3})$^{1/2}$

Figure S12 shows the calculated HOMO and LUMO + 1 of **1b** in the ground state. The geometry optimisation of the ground state of **1b** was performed at the Density Functional Theory level, using the CAM-B3LYP functional and the LANL2DZ basis set. The HOMO is spread symmetrically across the whole compound. The LUMO + 1 is more asymmetric and shifted to one side of the compound. The 10 lowest electronic transitions of **1b** are shown in **Figure S14**. The stick spectra, shown in black, have been convoluted with a Gaussian to produce the predicted spectra shown in blue. The predicted spectra and the measured UV/vis spectra of **1b**, shown in **Figure S5**, are in good agreement. The calculations show that the main transition at 362 nm is HOMO → LUMO + 1.

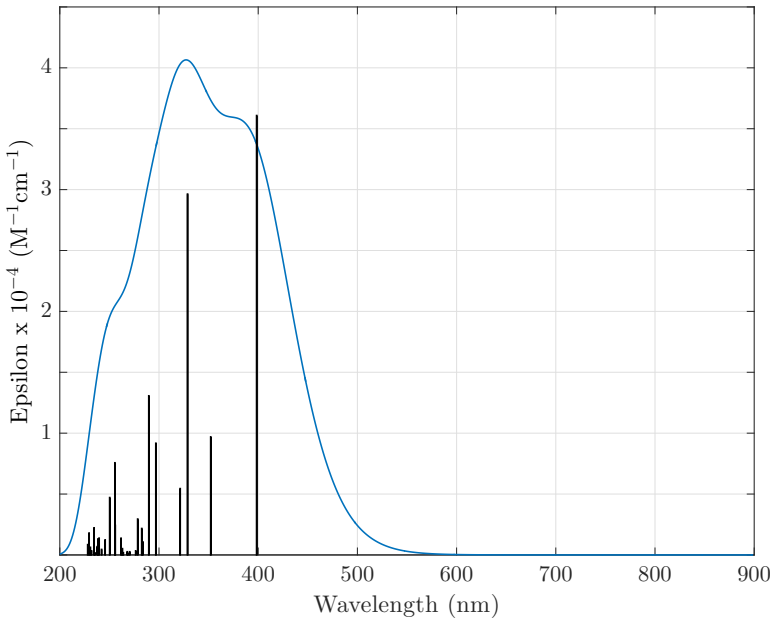

Figure S13: DFT-calculated 30 lowest electronic transitions (black stick spectrum) of **1a**. The 400 nm transition primarily belongs to HOMO → LUMO). The predicted UV/vis spectrum is shown in blue.

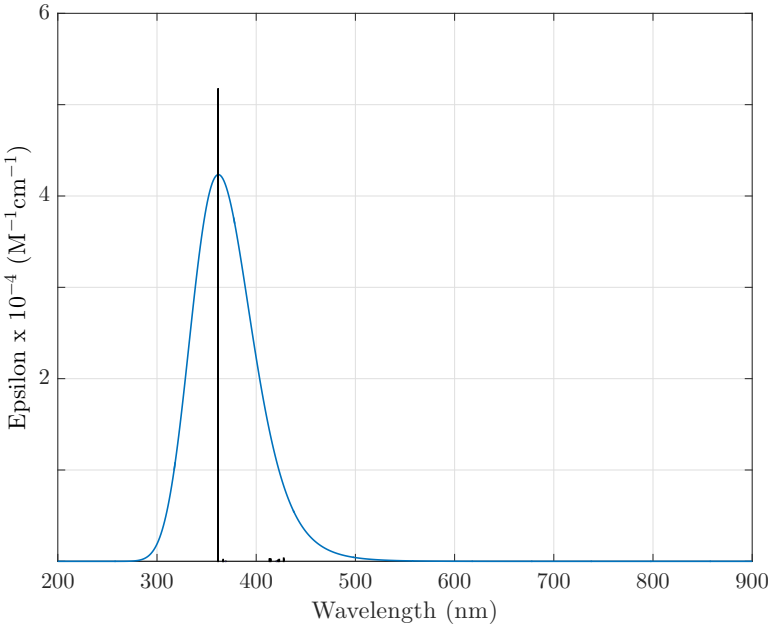

Figure S14: DFT-calculated 10 lowest electronic transitions (black stick spectrum) of **1b**. The 362 nm transition primarily belongs to HOMO $\rightarrow$ LUMO + 1). The predicted UV/vis spectrum is shown in blue.

Table S1: The bond lengths from the DFT and TD–DFT calculations of the Ground (GS), Singlet (S) and Triplet (T, time - dependent) states for each bond labeled in **Figure 1**. The GS - S and GS - T columns show the difference between the bond lengths of **1a** in the Singlet or Triplet state compared with the Ground State, respectively. The differences in bond lengths relate to the differences in the structure of **1a** seen in **Figure 1** (GS) and **Figure 8** (S and T).

Bond Lengths of **1a** (Å)					
Bond	GS	S	T	GS - S	GS - T
$Si_1 - C_{11}$	1.84807	1.84397	1.84782	0.0041	0.00025
$C_{11} - C_{12}$	1.22371	1.23262	1.23509	-0.00891	-0.01138
$C_{12} - C_{13}$	1.40887	1.38846	1.38062	0.02041	0.02825
$Si_2 - C_{21}$	1.84919	1.84679	1.84941	0.0024	-0.00022
$C_{21} - C_{22}$	1.22332	1.22901	1.23172	-0.00569	-0.0084
$C_{22} - C_{23}$	1.40922	1.39552	1.38761	0.0137	0.02161
$Si_3 - C_{31}$	1.84708	1.84783	1.84797	-0.00075	-0.00089
$C_{31} - C_{32}$	1.2238	1.22749	1.22429	-0.00369	-0.00049
$C_{32} - C_{33}$	1.40917	1.39921	1.40761	0.00996	0.00156
$C_{13} - C_{14}$	1.37988	1.40685	1.42682	-0.02697	-0.04694
$C_{14} - C_{15}$	1.42376	1.392	1.37289	0.03176	0.05087
$C_{15} - C_{16}$	1.38682	1.43784	1.47323	-0.05102	-0.08641
$C_{23} - C_{24}$	1.39414	1.44741	1.47253	-0.05327	-0.07839
$C_{24} - C_{25}$	1.42985	1.41274	1.38745	0.01711	0.0424
$C_{25} - C_{26}$	1.37679	1.38628	1.41135	-0.00949	-0.03456
$C_{33} - C_{34}$	1.38423	1.40868	1.3899	-0.02445	-0.00567
$C_{34} - C_{35}$	1.42557	1.40826	1.42109	0.01731	0.00448
$C_{35} - C_{36}$	1.37911	1.39245	1.38263	-0.01334	-0.00352
$C_{16} - C_{26}$	1.45675	1.4011	1.37707	0.05565	0.07968
$C_{25} - C_{36}$	1.46938	1.43798	1.45901	0.0314	0.01037

S5. Global Fitting for the Nanosecond Transient Absorption Spectra

Here is the model used to fit the spectra from the nanosecond visible transient absorption measurements visualised in **Figures 4** and **9**. Global analysis of the whole transient data matrix, assuming a sum of exponential time profiles and triplet-triplet annihilation was performed, using the model below:

$$a/(b * T + c) + d * exp(-T/\tau) \tag{S1}$$

Here T represents time, τ decay lifetime, and the other coefficeints are concentration dependent. The first component models the triplet-triplet annihilation and the second component models the T $\rightarrow$ GS transition, using a single exponential.

S6. NMR & NOESY Spectra of 1a

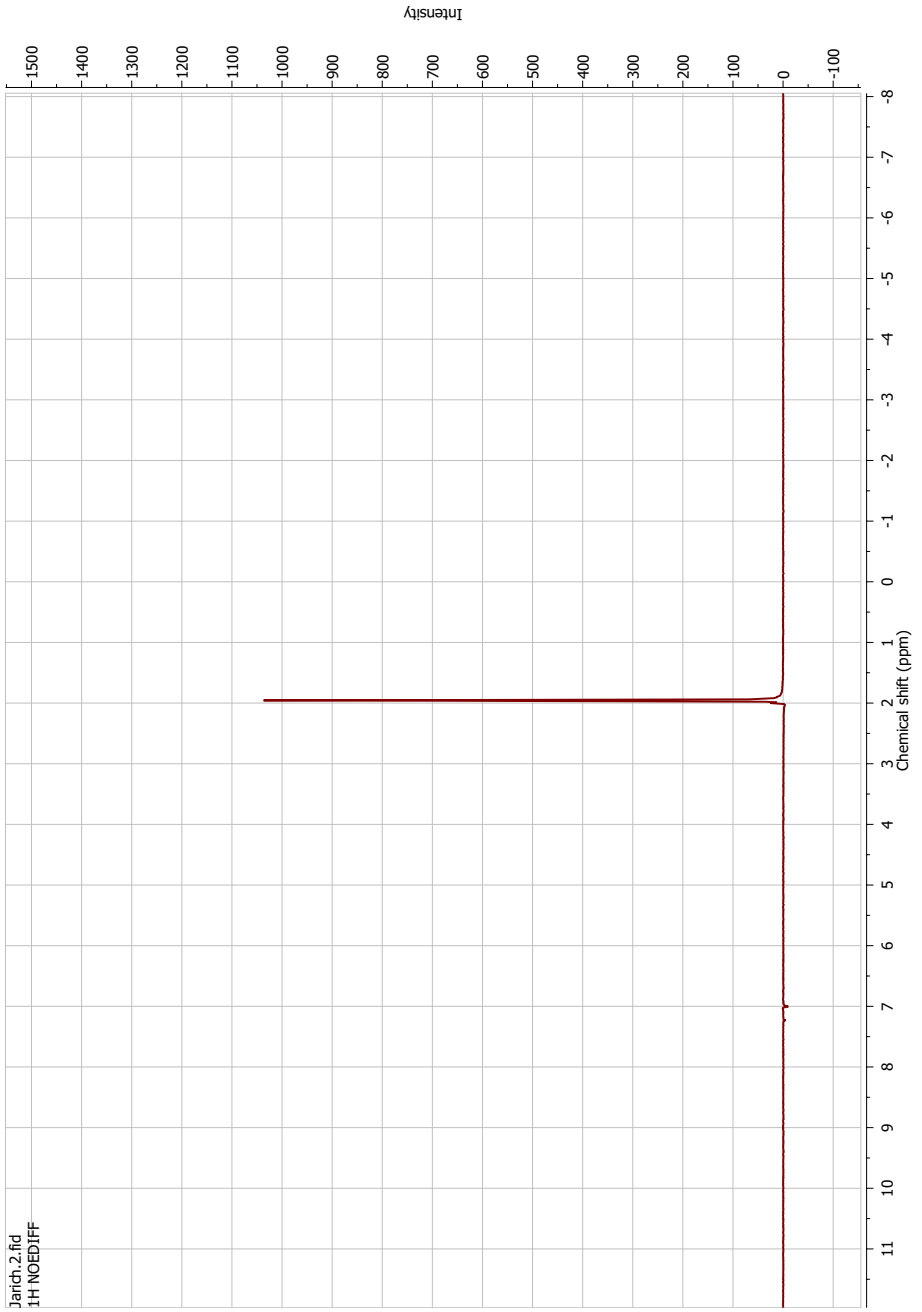

Figure S15: ^{1}H NOESY spectrum (recorded on a Bruker Advance ARX 400, 400 MHz) of **1a** in DCM-d_2 (purchased from Euriso-top) pulsed at 1.9 ppm, with no evidence of NOE resonance (see elsewhere), demonstrating that the methyl groups at the terthiophene core are distant and therefore in the anti-parallel conformation.

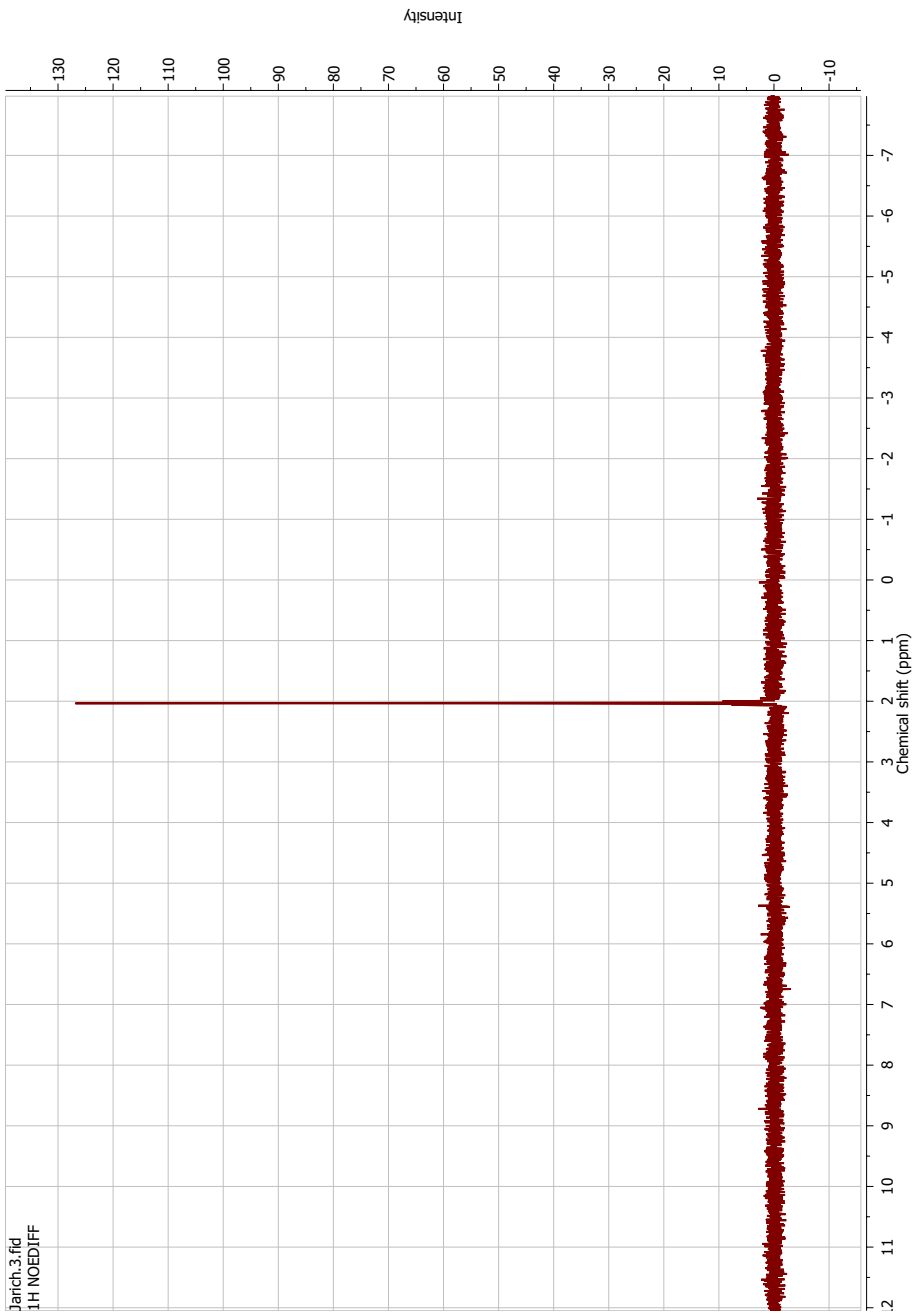

Figure S16: ^{1}H NOESY spectrum (recorded on a Bruker Advance ARX 400, 400 MHz) of **1a** in DCM-d_2 (purchased from Euriso-top) pulsed at 2.1 ppm, with no evidence of NOE resonance (see elsewhere), demonstrating that the methyl groups at the terthiophene core are distant and therefore in the anti-parallel conformation.

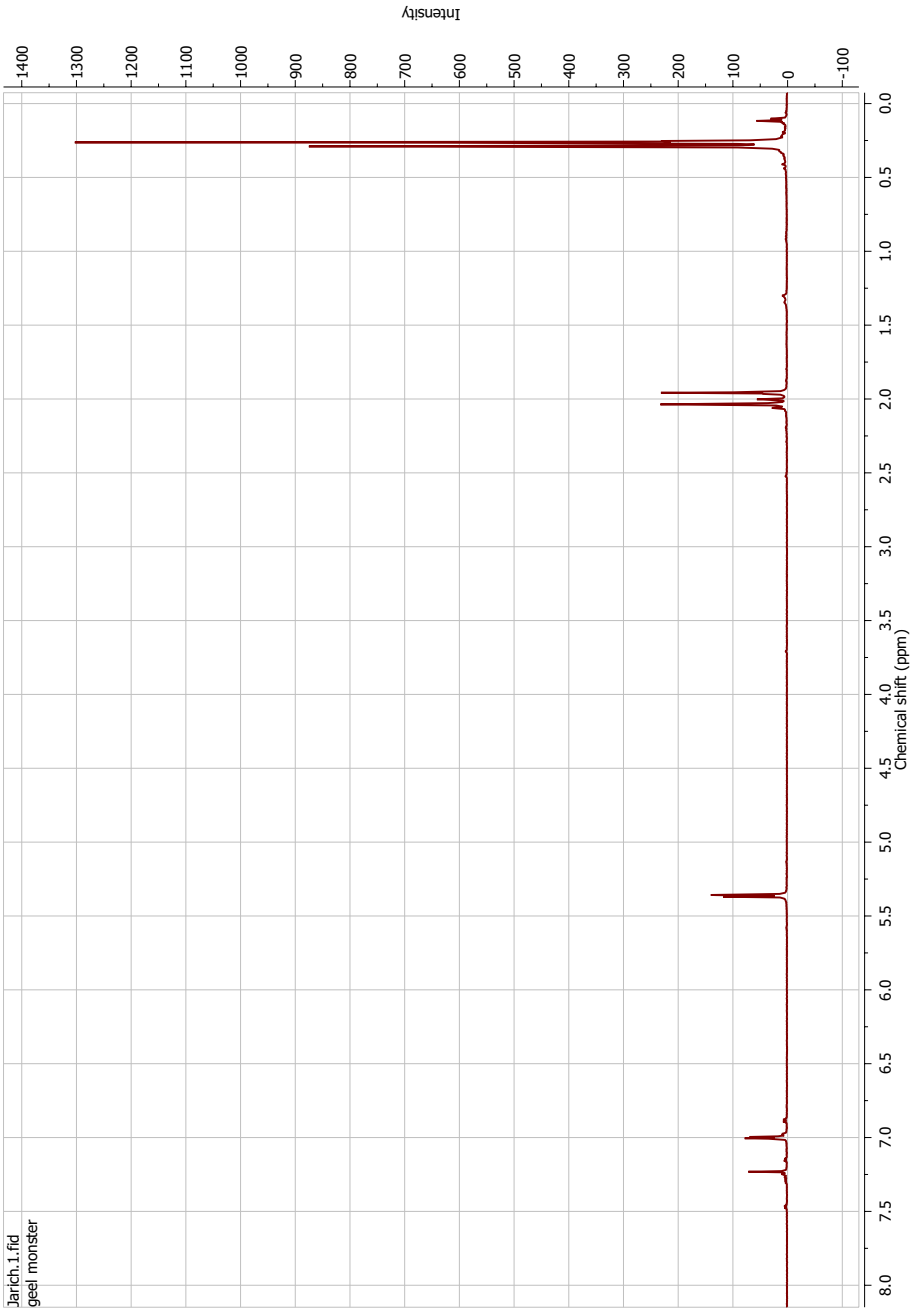

Figure S17: ^{1}H NMR spectrum (recorded on a Bruker Advance ARX 400, 400 MHz) of **1a** in DCM-d_2 (purchased from Euriso-top).

S7. Femtosecond Transient Absorption Spectra of 1b in THF

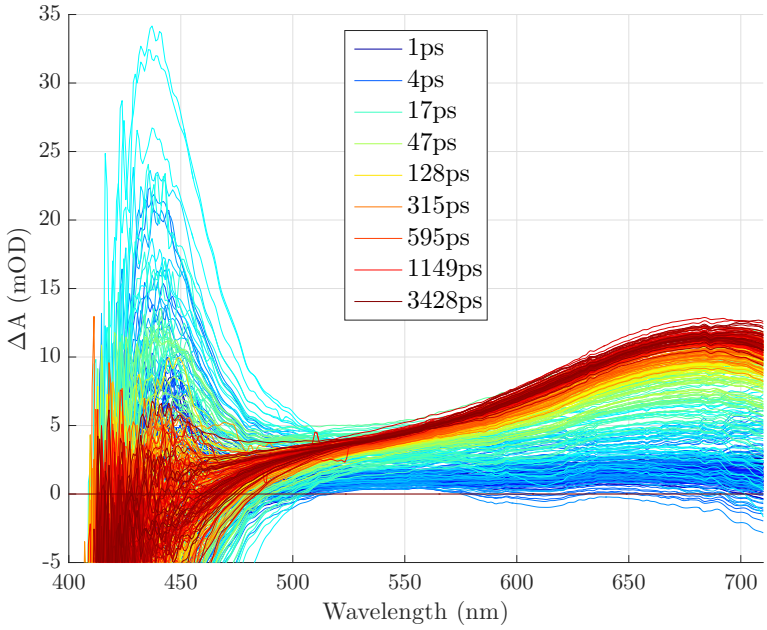

Figure S18: Femtosecond visible transient absorption spectra of **1b** in THF, excited at ca. 400 nm.

References

[S1] Zhang, J.; Sun, C.-F.; Zhang, M.-X.; Hartl, F.; Yin, J.; Yu, G.-A.; Rao, L.; Liu, S. H. Asymmetric oxidation of vinyl- and ethynyl terthiophene ligands in triruthenium complexes. *Dalton Trans.* **2016**, *45*, 768–782.